

# Annealing Temperatures' Effects on Microstructure and Optical Properties of Ba<sub>0.95</sub>Sr<sub>0.05</sub>TiO<sub>3</sub> Films

Y. Iriani<sup>1\*</sup>, F. Nurosyid<sup>1</sup>, R. Mayasari<sup>1</sup> and D. K. Sandi<sup>1</sup>

<sup>1</sup> Physics Department, Faculty of Mathematics and Natural Sciences, Universitas Sebelas Maret, Surakarta 57126, Indonesia

**ABSTRACT** – Ferroelectric materials, one of which is Barium Strontium Titanate (BST), can be applied for photovoltaic. Ferroelectric films function as the P-type semiconductor in the P-N junction. BST (Ba<sub>0.95</sub>Sr<sub>0.05</sub>TiO<sub>3</sub>) films have been deposited on Pt/Si (111) and quartz substrates via the CSD method prepared by spin coater. The films were annealed at various temperatures of 800°C, 900°C, and 1000°C to observe the annealing temperatures' effects on the microstructure and optical properties of the BST films. From the XRD results, the intensity of diffraction peaks gets higher along with the higher annealing temperature. It thus causes the level of crystallization and the crystal size of the Ba<sub>0.95</sub>Sr<sub>0.05</sub>TiO<sub>3</sub> films to increase. The morphology results reveal that the grains size of the Ba<sub>0.95</sub>Sr<sub>0.05</sub>TiO<sub>3</sub> films is getting larger with the higher annealing temperature. The optical properties examined in the Ba<sub>0.95</sub>Sr<sub>0.05</sub>TiO<sub>3</sub> films include absorbance and bandgap energy values. Values of bandgap energy show a decrease with increasing sintering temperature. The smallest bandgap energy of the Ba<sub>0.95</sub>Sr<sub>0.05</sub>TiO<sub>3</sub> film is achieved at 1000°C of 3.20 eV. BST films were annealed at temperature 1000°C attained from this study can be considered as candidate for a photovoltaic ferroelectric material.

## ARTICLE HISTORY

Received: 28 June 2021

Revised: 20 October 2021

Accepted: 27 October 2021

## KEYWORDS

Ba<sub>0.95</sub>Sr<sub>0.05</sub>TiO<sub>3</sub> films

Annealing Temperature

Microstructure

Optical properties

## INTRODUCTION

Perovskite solar cells (PSCs) have attracted the broad attention of the scientific community because of their fascinating features in the field of photovoltaic devices. It is a perovskite film sandwiched in a solar cell that acts as a photon absorber [1, 2]. It is low production costs, high absorption coefficient of light, high mobility, and adjustable bandgap [3, 4]. The photovoltaic effects in perovskite ferroelectrics occur inside the materials by exploiting the internal electric field to promote charge separation and electron transport [5, 6]. The internal electric field is originated from the spontaneous polarization and domains of the materials themselves [1, 3, 5]. Photovoltaic effects have been many studied in ferroelectric perovskites including BiFeO<sub>3</sub> [1, 5], Pb(Zr,Ti)O<sub>3</sub>, Nd-doped BTO [7], BTO [2-4, 8], and BST [9] where the current study reported efficiency of up to 21% [10].

In this study, BST is expected to be applied as a potential ferroelectric material in photovoltaic devices. The BST is easy to use because it has more stable chemical and mechanical characteristics and nearer Curie temperature to the room temperature than other ferroelectric materials [9, 11, 12]. Moreover, the BST also possesses relatively low bandgap energy, which is minimum photon energy to drive electrons from the valence to the conduction band [9].

Usually, BST films can be synthesized by pulsed laser deposition (PLD), radio frequency (RF) magnetron sputtering [13], metal-organic chemical vapor deposition (MOCVD), vacuum evaporation [14], molecular beam epitaxy (MBE) [15], and chemical solution deposition (CSD) [8, 16, 17] methods. Among these methods, the sol-gel method is most desirable by researchers because it is a simple and easy process, cost-effective, easy composition control, good homogeneity achieved, and low annealing temperature [8, 16-18].

Further, the films' properties are influenced by several deposition parameters one of which is annealing temperature. The annealing temperature has a significant action in the formation of BST film properties primarily on its basic structural and morphological properties. Meanwhile, the role of BST films in photovoltaic devices can be governed by several fundamental properties including the structural, morphological, and optical properties such as crystal size, micro-strain, grain size, refractive index, absorption, and bandgap [14]. It is crucial to study how the annealing temperature influence these properties because there is a relationship between the optical properties and the crystal structure also the morphology of the BST films. Moreover, less work has been done on the study related to this matter on BST film. Therefore, this study presents the investigation of the synthesis of the BST films by the CSD method and their microstructural, morphological, and optical properties at various annealing temperatures.

## EXPERIMENTAL METHOD

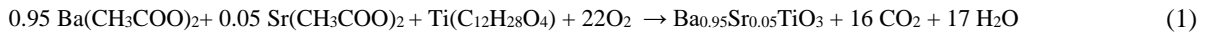
### Materials and Instruments

Here, the preparation of the Ba<sub>0.95</sub>Sr<sub>0.05</sub>TiO<sub>3</sub> films employed the CSD method. The starting materials for the manufacture were Barium Acetate Ba(CH<sub>3</sub>COO)<sub>2</sub>, Titanium Isopropoxide Ti(OC<sub>3</sub>H<sub>7</sub>)<sub>4</sub>, and Strontium Acetate Sr(CH<sub>3</sub>COO)<sub>2</sub> while Acetic Acid (CH<sub>3</sub>COOH) and Ethylene Glycol (HOCH<sub>2</sub>CH<sub>2</sub>OH) were the solvents.

The equipment used in this study involved X-Ray Diffractometer (XRD) to determine the crystal structure, Scanning Electrons Microscopy (SEM) to find out particles or grains size distribution, and UV-Spectrophotometry to investigate their optical properties.

### Method and Procedure

Firstly, the solutions of BST were made by mixing the starting materials and the solvents. Barium Acetate and Strontium Acetate were dissolved in Acetic Acid by stirring using a magnetic stirrer on a hot plate. Titanium Isopropoxide was then added and the stirring process was continued. Ethylene Glycol was lastly poured and stirred. The solutions were further heated for 1 h until homogeneous BST solutions were obtained. Finally, the solutions were deposited on the Pt/Si and quartz substrates via the spin coating technique with a rotating speed of 3000 rpm. The films were dried then followed by annealing process at varied temperatures of 800°C, 900°C, and 1000°C with a heating rate of 5°C/min for 5 h. The chemical reactions occurred during the manufacture of the BST solutions were as follows.



The films were then characterized by XRD to determine the crystal structure with the Cu X-Ray ( $\lambda=1.5406 \text{ \AA}$ ). The XRD patterns were then exploited to estimate the crystallinity level and crystallite size through Eq. 2 and Eq. 3, respectively.  $D$  was crystallite size,  $k$  was Scherer constant,  $\lambda$  was the wavelength,  $\beta$  was Full-Width Half Maximum (FWHM) and  $\theta$  was the diffraction angle [9]. Finally, the films' morphology was examined by Scanning Electrons Microscopy (SEM) and UV-Spectrophotometry.

$$D = k \lambda / \beta \cos \theta \quad (2)$$

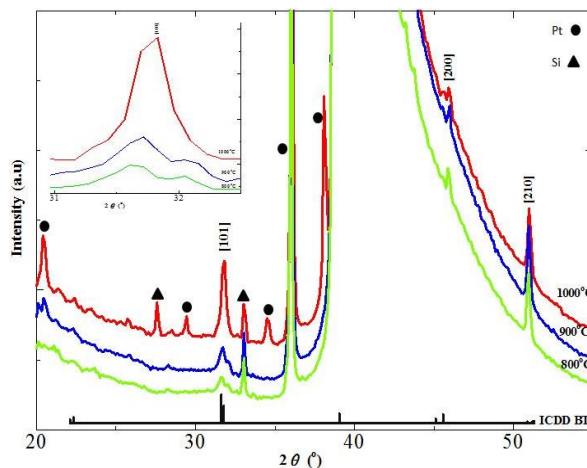
$$\text{Crystallinity (\%)} = \frac{\text{Int}_{\text{Max}}}{\text{Int}_{\text{Max}} + \text{Int}_{\text{Min}}} \times 100\% \quad (3)$$

## RESULT AND DISCUSSION

The BST ( $\text{Ba}_{1-x}\text{Sr}_x\text{TiO}_3$ ) films with a concentration of 0.6 M and  $x=5\%$  have been successfully deposited on Pt/Si (111) and quartz substrates with various annealing temperatures of 800°C, 900°C, and 1000°C. Figure 1 presents the XRD patterns of the BST films at different annealing temperatures. The patterns have been compared and agree with ICDD database of  $\text{BaTiO}_3$  (#831880) revealing tetragonal crystal structures of the  $\text{Ba}_{0.95}\text{Sr}_{0.05}\text{TiO}_3$  films at all temperatures. Besides, there are other phases exhibiting the existence of the Pt/Si(111) substrates which matches with ICDD database numbers of #011190 (Pt) and #721088 (Si).

Based on Figure 1, the effect of the annealing temperature on the intensity of the diffraction is very significant that is seen on the main peak of (101) which reveals the higher the intensity as the higher temperature. The annealing process with high temperatures causes atomic vibrations in the material so that the atoms will be arranged regularly in a certain crystal plane orientation [20]. This leads to the more X-Ray rays diffracted and captured by the detector which means the higher intensity is detected. Furthermore, the higher intensity indicates the larger crystallinity level of materials.

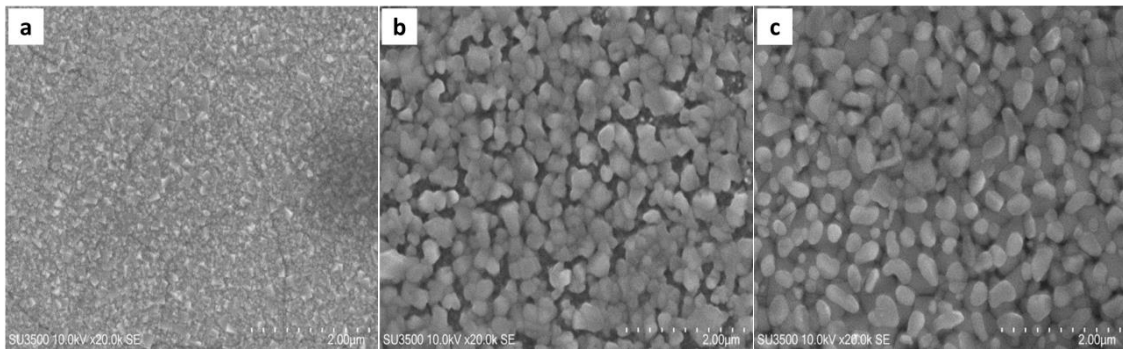
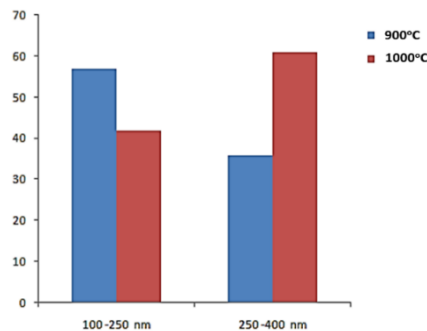
Table 1 displays crystallinity level/ degree, lattice parameter, and crystallite size of the BST films at various annealing temperatures. The lattice parameters of the BST films were obtained from the refinement process (Rietveld Method) using GSAS software. The refinement process reveals that the lattice of the films are getting larger with the higher sintering temperature and the increment is majorly located in the  $c$  lattice. Additionally, in accordance with the lattice, the crystallite



**Figure 1.** Diffraction patterns of the  $\text{Ba}_{0.95}\text{Sr}_{0.05}\text{TiO}_3$  at different annealing temperatures

**Table 1.** Lattice parameter, crystallinity degree, and crystallite size of the  $\text{Ba}_{0.95}\text{Sr}_{0.05}\text{TiO}_3$  films at various annealing temperatures

Annealing temperature	Lattice Parameters ( $\text{\AA}$ )		Crystallinity degree (%)	Crystallite size (nm)
	a=b	c		
800°C	3.994	4.041	77.48	20.55
900°C	3.995	4.083	86.39	25.95
1000°C	3.995	4.085	89.27	27.16

**Figure 2.** Morphology images of the  $\text{Ba}_{0.95}\text{Sr}_{0.05}\text{TiO}_3$  films at (a) 800°C, (b) 900°C, and (c) 1000°C.**Figure 3.** Particles size distribution of the  $\text{Ba}_{0.95}\text{Sr}_{0.05}\text{TiO}_3$  films at 900°C and 1000°C

size is greater with the higher sintering temperatures either. For this reason, the higher sintering temperatures deliver higher energy received by atoms to diffuse and agglomerate which leads to the larger lattice parameters and crystallite size [14].

Table 1 displays crystallinity level/ degree, lattice parameter, and crystallite size of the BST films at various annealing temperatures. The lattice parameters of the BST films were obtained from the refinement process (Rietveld Method) using GSAS software. The refinement process reveals that the lattice of the films was getting larger with the higher sintering temperature and the increment is majorly located in the c lattice. Additionally, in accordance with the lattice, the crystallite size is greater with the higher sintering temperatures either. For this reason, the higher sintering temperatures deliver higher energy received by atoms to diffuse and agglomerate which leads to the larger lattice parameters and crystallite size [14].

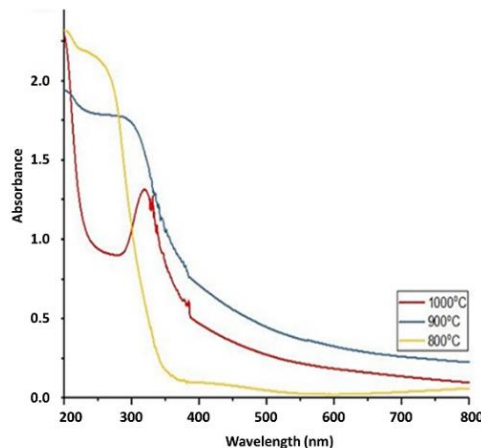
The morphology images of the  $\text{Ba}_{0.95}\text{Sr}_{0.05}\text{TiO}_3$  films for the annealing temperature variation are shown in Figure 2. At 800°C the grain boundaries are not visible because the grains might be very fine in such magnification so that the grain size in this part could not be measured. Meanwhile, at 900°C and 1000°C, the grain boundaries are visible and the effects of annealing temperatures could be observed.

Figure 3 presents the grain size distribution for the BST films at 900°C and 1000°C. The grain size of the BST films at 900°C is in the range of 100-250 nm while it is in the range of 250-400 nm at 1000°C. Therefore, it can be concluded that the grain size increases with increasing annealing temperatures. This is because the higher annealing temperature could rise the diffusion process between the grains. This result is in accordance with the research conducted in [21].

Table 2 presents the thickness of the  $\text{Ba}_{0.95}\text{Sr}_{0.05}\text{TiO}_3$  films at all annealing temperatures. Based on the table, the films' thickness decreases as the increase in the annealing temperatures which is inversely proportional to the grain size. Since the films were made of the acetic solvents with the boiling point of  $\sim 125^\circ\text{C}$ , the higher temperatures could cause reduction in the films' mass leading to compactness and a decrease in thickness. The thickness values were further exploited to estimate the bandgap values of the  $\text{Ba}_{0.95}\text{Sr}_{0.05}\text{TiO}_3$  films based on the Eq. 5.

**Table 2.** Thickness of the Ba<sub>0.95</sub>Sr<sub>0.05</sub>TiO<sub>3</sub> films at various annealing temperatures

Annealing temperatures	Thickness (nm)
800°C	556
900°C	424
1000°C	236

**Figure 4.** Absorbance spectra of the Ba<sub>0.95</sub>Sr<sub>0.05</sub>TiO<sub>3</sub> films

Next, Figure 4 is the absorbance spectra of the Ba<sub>0.95</sub>Sr<sub>0.05</sub>TiO<sub>3</sub> films at the various annealing temperature. It can be seen that the higher the temperature induces the smaller absorbance spectra. Besides, the absorbance peak also shifts to the right (towards the visible area) [21].

The highest absorbance value is at a temperature of 800°C. The absorbance value increases at 200-400 nm wavelength. The Ba<sub>0.95</sub>Sr<sub>0.05</sub>TiO<sub>3</sub> films can absorb sunlight well in UV areas. However, it does not work well in the visible region because the absorbance is constant [5].

The calculation of the energy value of the bandgap uses the Tauc-plot method using the following equations.  $d$  is the film thickness,  $\alpha$  is the absorbance coefficient as a function of photon energy ( $m^{-1}$ ),  $E_g$  is the bandgap energy (eV),  $C$  is the material constant,  $h$  is the Planck constant ( $6.626 \times 10^{-34}$  Js or  $4.14 \times 10^{-15}$  eV.S),  $\lambda$  is the wavelength (nm), and  $\nu$  is the frequency of the wave (Hz) [21].

$$\alpha h\nu = C(h\nu - E_g)^n \quad (4)$$

$$\nu = c/\lambda \quad (5)$$

$$\alpha = -\frac{1}{d} \ln T \quad (6)$$

Figure 5 exhibits the bandgap energy of the Ba<sub>0.95</sub>Sr<sub>0.05</sub>TiO<sub>3</sub> films those are 3.81 eV, 3.66 eV and 3.20 eV for annealing temperatures of 800°C, 900°C and 1000°C, respectively. These results are consistent with research conducted in [18]. The bandgap energy is influenced by the microstructure of the films in which the microstructure itself can be strongly affected by the annealing temperature during fabrication. Lower bandgap energies indicate increased crystallinity and homogeneity of the layers [18]. The other reasons might come from the increase in the lattice parameter and crystallite size. It is on several reports that in the non-thin film, the thickness did not affect the bandgap, however, the larger crystallite size lead to the higher bandgap values due to there is a quantum confinement effect [21-23]. Thus, since the higher sintering cause the larger crystallite size, it thus could lower the bandgap energy.

When it is applied to solar cells, the Ba<sub>0.95</sub>Sr<sub>0.05</sub>TiO<sub>3</sub> with small bandgap energy will accelerate the transfer of electrons from the conduction band gap to the valence band gap [7]. Therefore, due to the optimal microstructure and morphological properties so that the lowest bandgap is obtained, the BST film at 1000°C can be considered a good candidate for photovoltaic ferroelectric material that further research related to photovoltaic properties can be carried out on this material.

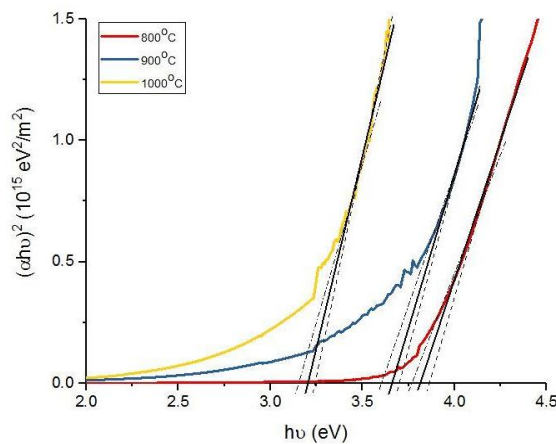


**Figure 5.** Tauc-plot for bandgap energy estimation of the  $\text{Ba}_{0.95}\text{Sr}_{0.05}\text{TiO}_3$  films

## CONCLUSION

The  $\text{Ba}_{0.95}\text{Sr}_{0.05}\text{TiO}_3$  films on Pt/Si (111) and quartz substrates have been successfully grown using the CSD process. The XRD results show the higher the intensity peak of the  $\text{Ba}_{0.95}\text{Sr}_{0.05}\text{TiO}_3$  films as the higher the temperature. The higher temperature also causes a higher crystallinity level and a larger crystallite size. The optical properties of the  $\text{Ba}_{0.95}\text{Sr}_{0.05}\text{TiO}_3$  films including the absorbance and the bandgap energy exhibit that the absorbance value and thus the band gap energy decrease with increasing temperature. The smallest bandgap energy is obtained by the  $\text{Ba}_{0.95}\text{Sr}_{0.05}\text{TiO}_3$  annealed at 1000°C. Hence, it can be concluded that the  $\text{Ba}_{0.95}\text{Sr}_{0.05}\text{TiO}_3$  annealed at 1000°C is the best perovskite material obtained from this study so that it can be a good candidate for solar cells or photovoltaic application. (TNR 10) Conclusions are written in paragraph forms without numbering or indenting.

## ACKNOWLEDGEMENT

The authors would like to thank Kementerian Pendidikan, Kebudayaan, Riset, dan Teknologi for financial support through Penelitian Dasar with a contract number of 112/UN27.21/HK/2020.

## REFERENCES

- [1] C.L. Fu, W. Cai, Z.B. Lin, and W. H. Jiang. "Photovoltaic Effects of Bismuth Ferrite and Nd-Doped Barium Titanate Thin Films Prepared by Sol-Gel Method." *Materials Science Forum*, vol. 787, pp. 347-351, 2014.
- [2] A.K. Sharma, B.G. Priyadarshini, B. R. Mehta, and D. Kumar. "An Amorphous Barium Titanate Thin Film Improves Light Trapping in Si Solar Cells." *RSC Advances*, vol. 5(74), pp. 59881-59886, 2015.
- [3] X. Luo, J. Ding, J. Wang, and J. Zhang. "Electron Transport Enhancement in Perovskite Solar Cell via the Polarized  $\text{BaTiO}_3$  Thin Film." *Journal of Materials Research*, vol. 35(16), pp. 2158-2165, 2020.
- [4] E. Scholtz, P. Šutta, P. Calta, P. Novák, M. Solanská, and J. Müllerová. "Investigation of Barium Titanate Thin Films as Simple Antireflection Coatings for Solar Cells." *Applied Surface Science*, vol. 461, pp. 249-254, 2018.
- [5] W. Cai, C. Fu, J. Gao, Q. Guo, X. Deng, and C. Zhang. "Preparation and Optical Properties of Barium Titanate Thin Films." *Physica B: Condensed Matter*, vol. 406(19), pp. 3583-3587, 2011.
- [6] B. Chen, X. Zheng, M. Yang, Y. Zhou, S. Kundu, J. Shi, K. Zhu, and S. Priya. "Interface Band Structure Engineering by Ferroelectric Polarization in Perovskite Solar Cells." *Nano Energy*, vol. 13, pp. 582-591, 2015.
- [7] W. Jiang, W. Cai, Z. Lin, and C. Fu. "Effects of Nd-Doping on Optical and Photovoltaic Properties of Barium Titanate Thin Films Prepared by Sol-Gel Method." *Materials Research Bulletin*, vol. 48(9), pp. 3092-3097, 2013.
- [8] A.U.L.S. Setyadi, Y. Iriani, and F. Nurosyid. "Optical Properties and Microstructure of Barium Titanate Thin Film ( $\text{BaTiO}_3$ ) for Solar Cell Applications." in *IOP Conference Series: Materials Science and Engineering*, 2018, pp. 333.
- [9] Irzaman, I.R. Putra, Aminullah, H. Syafutra, and H. Alatas. "Development of Ferroelectric Solar Cells of Barium Strontium Titanate ( $\text{Ba}_x\text{Sr}_{1-x}\text{TiO}_3$ ) for Substituting Conventional Battery in LAPAN-IPB Satellite (LISAT)." *Procedia Environmental Sciences*, vol. 33, pp. 607-614, 2016.
- [10] H. Wang, R. Jiang, M. Sun, X. Yin, Y. Guo, M. He, and L. Wang. "Titanate Hollow Nanospheres as Electron-Transport Layer in Mesoscopic Perovskite Solar Cell with Enhanced Performance." *Journal of Materials Chemistry C*, vol. 7(7), pp. 1948-1954, 2019.
- [11] J. Iskandar, R.P. Jenie, U.J. Siregar, B. Yuliarto, and Irzaman. "Application of Thin Film Barium Strontium Titanate (BST) in a Microcontroller Based Tool to Measure Oxygen Saturation in Blood." *Ferroelectrics*, vol. 554(1), pp. 134-143, 2020.
- [12] M. Y. Shahid, F. Malik, M. Asghar, M. F. Warsi, and S. Z. Ilyas. "Effect of Sr-Doping on Ferroelectric and Dielectric Properties of Sol-Gel Synthesized  $\text{BaTiO}_3$  Thin Films." *Digest Journal of Nanomaterials and Biostructures*, vol. 12(3), pp. 669-677, 2017.
- [13] J. Li, C.C. Zhang, Y.L. Wang, Y. Gao, and X. L. Zhao. "Radio Frequency (RF) Magnetron Sputtered Barium Strontium Titanate (BST) Thin Film." *Key Engineering Materials*, vol. 727, pp. 942-946, 2017.

- [14] R. Sengodan, R. Balamurugan, and B. Chandra Shekar. "Temperature Dependence on Optical Properties of Sr Doped BaTiO<sub>3</sub> Thin films by Vacuum Evaporation Method." *International Journal of Thin Film Science and Technology*, vol. 8, pp. 147-156, 2019.
- [15] C.J.G. Meyers, C.R. Freeze, S. Stemmer, and R. A. York. "Effect of BST Film Thickness on The Performance of Tunable Interdigital Capacitors Grown by MBE." *Applied Physics Letters*, vol. 111(26), 2017.
- [16] Y.C. Teh, N.R. Ong, Z. Sauli, J.B. Alcain, and V. Retnasamy. "Barium Strontium Titanate (BST) Thin Film Analysis on Different Layer and Annealing Temperature, in *AIP Conference Proceedings*, 2017.
- [17] R.T. Setyadhani, A. Jamaludin, and Y. Iriani. "Effects of Iron Dopants on Barium Strontium Titanate (Ba<sub>0.8</sub>Sr<sub>0.2</sub>TiO<sub>3</sub>) Thin Films." *Advanced Materials Research*, vol. 896, pp. 229-232, 2014.
- [18] Y. Xu and M. Shen. "Structure and Optical Properties of nanocrystalline Bifeo<sub>3</sub> Films Prepared by Chemical Solution Deposition." *Materials Letters*, vol. 62(20), pp. 3600-3602, 2008.
- [19] M.M. Vijatovic, J. D. Bobic, and B. D. Stojanovic. "History and Challenges of Barium Titanate: Part I." *Science of Sintering*, vol. 40(2), pp. 155-165, 2008.
- [20] D. K. Sandi, A. Supriyanto, A. Jamaluddina, and Y. Iriani. "The Effects Of Sintering Temperature on Dielectric Constant of Barium Titanate (BaTiO<sub>3</sub>)." in *IOP Conference Series: Materials Science and Engineering*, , 2016, vol. 107.
- [21] H.Y. D. Bao, L. Zhang, and X. Yao. "Structure and Optical Properties of SrTiO<sub>3</sub> Thin Films Prepared by a Sol-Gel Technique." *Physica Status Solidi*, vol. 169, pp. 227-233, 1998.